Journal of Sound and Vibration (1994) **178**(5), 591–605

FLEXIBLE ROTATING BEAM: COMPARATIVE MODELLING OF ISOTROPIC AND COMPOSITE MATERIAL INCLUDING GEOMETRIC NON-LINEARITY

C. I. CHEN† AND V. H. MUCINO

Mechanical and Aerospace Engineering Department

AND

C. C. SPYRAKOS

Civil Engineering Department, West Virginia University, Morgantown, West Virginia 26505, *U.S.A.*

(*Received* 11 *December* 1991, *and in final form* 26 *July* 1993)

A comparative modelling of a flexible rotating beam has been considered in this study. The dynamic model is based on a beam with either isotropic material or composite material. The composite beam is considered as orthotropic fiber-reinforced and symmetrically laminated. Both small linear as well as geometric non-linear deformations are studied.

A continuous system is considered in the analytical approach. Both axial and transverse deformations are included, and they are represented by the mode shape functions of the beam. The coupled effect between the rigid body motion and the flexible motion is also considered. A forward dynamic numerical simulation is performed for a prescribed driving torque on a steel and graphite/epoxy beam. The influence of flexibility on the rigid body motion is presented and discussed. From the numerical results, the composite material has a lower energy consumption due to lower material density. It performs well in damping the vibration of the structure due to its higher stiffness-to-weight ratio.

1. INTRODUCTION

Dynamic modelling of flexible mechanical systems has arisen in the past two decades. In advanced machine design, accurate models for studying elastic deformations and rigid motion of continuous, elastic bodies are becoming increasingly important. The problem of an elastic appendage on a rotating base is the simplest model in the study of beam-like structural dynamic analysis. Although the model is simple, it has initiated many research investigations. The analysis of free vibration characteristics of a rotating beam has been studied in references [1–5]. Most of these analytical studies place the emphasis on the critical speed. Other applications of the rotating flexible beam are one-link robotic manipulator systems [6–10], where the emphasis is based on predicting the deflections at the end of the manipulator. Furthermore, flexible beam elements in flexible multi-body mechanical systems can be categorized as another group of problems [11–14], such as the open loop chain system and closed loop mechanisms.

†Now with Chung-Hua Polytechnic Institute, Hsin Chu, Taiwan 300.

0022–460X/94/500591 + 15 $08.00/0

Two types of methodologies have been developed for the dynamic analysis in this area: in the first one, an analytical technique [15–19] solves separately for rigid motion and elastic deformation. The fundamental assumption in this approach is that small elastic motion is initially considered to have no effect on the rigid body motion. Inertial forces developing from the rigid motion play a dominant role in the flexible motion. The overall configuration is derived by superimposing the flexible response on the rigid body motions. This is not an accurate model when the mechanical system is subjected to high speeds. In the second methodology, a more accurate model [14] couples the rigid body motion and flexible motion. Rigid body motion and elastic deformations are solved simultaneously.

Generally speaking, research in this area can be divided into two categories. The first treats the elastic links of the mechanical system as a continuous system [20–24]. The equations of motion for these continuous systems are derived with the help of certain simplifying assumptions and solved to obtain the system response. In the second category, the elastic links of the system are modelled as discrete systems via finite element formulations [25–29]. The advantages of the finite element formulations are that they provide an easier and systematic modelling technique for complex mechanical systems. The drawback of the second method is the requirement of substantial computer time simulation due to the many degrees of freedom in the system. However, modal synthesis can be utilized to reduce the degrees of freedom. In addition, the accuracy of the dynamic response depends on the selection of the modal degrees of freedom [30, 31].

Most of the research done in this area is based on the assumption of small deformations of the flexible members, thus neglecting the effects of geometric non-linearity. The need to consider geometric non-linearity has prompted the development of many solution techniques for non-linear structural analysis. Geometric non-linearity occurs when the deflections are large enough to cause significant changes in the geometry of the structure. In some research, models have been developed that consider the geometric non-linearity in different mechanical systems [32–36]. However, most of these works do not evaluate for rigid motion and elastic motion simultaneously [32–34]. Bakr and Liou [35, 36] considered rigid body motion and flexible motion simultaneously in four bar and slider mechanism systems.

As mentioned before, most studies in this area consider the flexible bodies built with isotropic materials. Recently, an alternative philosophy has been proposed for the design of flexible multi-body systems which requires the members to be fabricated with advanced composite materials [37–43]. Generally speaking, composite materials possess much higher strength-to-weight and stiffness-to-weight ratios than those of metals. Consequently, systems made of composite materials experience much smaller deflections when subjected to loads.

This study pertains to the comparative modelling of a rotating flexible beam structure. The flexible beam is attached to a rotating base and the other end is free. The beam is considered with isotropic and composite material under the assumption of linearly small or geometrically non-linear deformation. There are four totally different models: linear deformation with isotropic material (LI), geometric non-linearity deformation with isotropic material (NLI), linear deformation with composite material (LCP) and geometric non-linearity deformation with composite material (NLCP). In order to consider the non-linear elastodynamic model of the system, the forward dynamic simulation is performed by applying a prescribed driving torque to a steel and to graphite/epoxy beam models. The responses of the transverse deformation and the influences of the flexibility on the rigid body motion are presented and discussed. It can be shown that the composite material has a lower energy consumption due to lower material density. It performs well in damping the vibration of the structure due to its higher stiffness-to-weight ratio.

2. ANALYTICAL BACKGROUND

The general analytical method of this type of problem has been well developed and proven to be suitable for analyzing mechanical systems subjected to kinematic constraints [14]. Two sets of generalized co-ordinates are employed to describe the configuration of the flexible body. One set are the reference generalized co-ordinates which define the location and orientation of a beam-fixed co-ordinate system on the beam, and the other set are the elastic co-ordinates which define the deformation of the beam with respect to the beam fixed co-ordinate system. The elastic deformations are introduced using the deformed shape functions and the time dependent generalized co-ordinates. The kinetic energy is obtained by integrating the kinetic energy of an infinitesimal element over the volume of the beam, while strain energy is derived in specific modelling. The quadratic terms in the strain-displacement relationship for linear small deformation are neglected. On the other hand, the quadratic terms are retained in the derivation of the strain energy for the geometric non-linear deformation. The equations of motion are derived through Lagrange's formulation [14]. Due to the coupled effect of rigid motion and elastic deformation, the equations of motion are non-linear, with time-dependent coefficients. Since the inverse dynamic analysis is impossible without simplifying the coupled effect, the forward dynamic simulation is implemented by a prescribed driving torque.

2.1. KINEMATICS

The configuration of the flexible beam system is illustrated in Figure 1. Let the X–Y co-ordinate system represent the inertial reference frame and the x–y system represent the beam-fixed co-ordinate frame. The global position of an arbitrary point P on the flexible beam can be expressed as

$$\mathbf{r}_p = \mathbf{A}_1 \bar{\mathbf{r}}, \tag{1}$$

where $\bar{\mathbf{r}}$ is the local position vector of point P in the deformed state (the bar represents the vector with respect to the beam-fixed co-ordinates system) and $\mathbf{A}_1$ is the transformation matrix, defined as

$$\mathbf{A}_1 = \begin{bmatrix} \cos\theta & -\sin\theta \\ \sin\theta & \cos\theta \end{bmatrix}. \tag{2}$$

The position vector $\bar{\mathbf{r}}$ can be written as

$$\bar{\mathbf{r}} = \bar{\mathbf{u}}_0 + \bar{\mathbf{u}}_f, \tag{3}$$

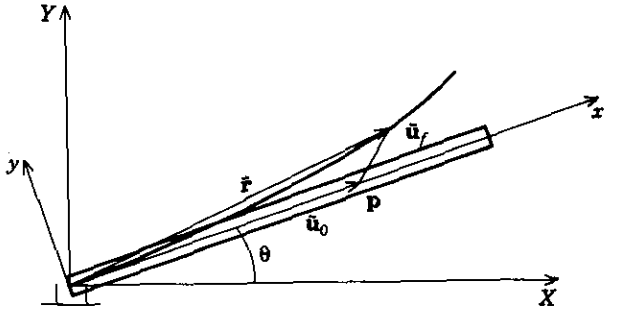

Figure 1. The general configuration of the flexible beam.

where $\bar{\mathbf{u}}_0$ is the position vector of point P in the undeformed state and $\bar{\mathbf{u}}_f$ is the deformed position vector of point P with respect to the beam-fixed co-ordinate. The deformed position vector $\bar{\mathbf{u}}_f$ can be represented by

$$\bar{\mathbf{u}}_f = \begin{Bmatrix} \bar{u} \\ \bar{v} \end{Bmatrix} = \begin{Bmatrix} \sum_{i=1}^{md} \Psi_{ai} q_{ai}(t) \\ \sum_{i=1}^{md} \Phi_{ti} q_{ti}(t) \end{Bmatrix}, \tag{4}$$

where $\bar{u}$ and $\bar{v}$ are the axial and transverse deformations, respectively, with respect to the x–y co-ordinates; Ψ_{ai} and Φ_{ti} are space-dependent shape functions and can be selected as the mode shape functions of the free axial and the free transverse vibration, respectively; $q_{ai}(t)$ and $q_{ti}(t)$ are the time-dependent elastic generalized co-ordinates of the deformable beam and md is the number of modes. Equation (4) can be written as

$$\bar{\mathbf{u}}_f = \begin{bmatrix} \psi_{a1} & \psi_{a2} & \cdots & \psi_{amd} & 0 & 0 & \cdots & 0 \\ 0 & 0 & \cdots & 0 & \phi_{t1} & \phi_{t2} & \cdots & \phi_{tmd} \end{bmatrix} \begin{Bmatrix} q_{a1} \\ q_{a2} \\ \vdots \\ q_{amd} \\ q_{t1} \\ q_{t2} \\ \vdots \\ q_{tmd} \end{Bmatrix}, \tag{5}$$

or, in a simplified form,

$$\bar{\mathbf{u}}_f = [\mathbf{S}]\{\mathbf{q}_f\} \tag{6}$$

where $[\mathbf{S}]$ is the shape matrix and $\{\mathbf{q}_f\}$ is the vector of the elastic generalized co-ordinates. The overall generalized co-ordinates of the beam can be expressed as

$$\{\mathbf{q}\} = \{\theta, \{\mathbf{q}_f\}^{\mathrm{T}}\}^{\mathrm{T}}, \tag{7}$$

where θ is the rigid angular displacement.

The velocity of an arbitrary point P can be obtained by differentiating equation (1) with respect to time,

$$\dot{\mathbf{r}}_p = \mathbf{L}_v\{\dot{\mathbf{q}}\}, \tag{8}$$

where $\{\dot{\mathbf{q}}\}$ is the generalized velocity vector of beam and $\mathbf{L}_v$ is defined as

$$\mathbf{L}_v = [\mathbf{B} \quad \mathbf{A}_1\mathbf{S}], \tag{9}$$

in which

$$\mathbf{B} = \begin{bmatrix} -\sin\theta & -\cos\theta \\ \cos\theta & -\sin\theta \end{bmatrix} \bar{\mathbf{r}}. \tag{10}$$

2.2. KINETIC ENERGY

The kinetic energy of the beam is given by

$$T = \tfrac{1}{2}\rho \int \dot{\mathbf{r}}_p^{\mathrm{T}} \dot{\mathbf{r}}_p \, \mathrm{d}V, \tag{11}$$

where ρ is the constant mass density and $\dot{\mathbf{r}}_p$ is the global velocity of an arbitrary point P on the beam. Substituting equation (8) into equation (11) yields

$$T = \tfrac{1}{2}\dot{\mathbf{q}}^{\mathrm{T}}\mathbf{M}\dot{\mathbf{q}}, \tag{12}$$

where

$$\mathbf{M} = \begin{bmatrix} m_{\theta\theta} & m_{\theta f} \\ m_{f\theta} & m_{ff} \end{bmatrix}, \tag{13}$$

and

$$m_{\theta\theta} = \rho \int \mathbf{B}^{\mathrm{T}}\mathbf{B}\,\mathrm{d}V, \qquad m_{\theta f} = \rho \int \mathbf{B}^{\mathrm{T}}\mathbf{A}_1 S\,\mathrm{d}V, \qquad m_{ff} = \rho \int \mathbf{S}^{\mathrm{T}}\mathbf{S}\,\mathrm{d}V. \tag{14}$$

In this study, the kinetic energy expression in equation (12) is the same for all cases under the assumption of constant mass density along the beam.

2.3. STRAIN ENERGY

The strain energy is not given by the same expression for the linear deformation and the geometric non-linear case. For linear deformation, the quadratic terms in the strain–displacement relationship are neglected. However, the quadratic terms have to be retained in considering geometric non-linearity. The strain energy is obtained for the linear and the non-linear cases, separately.

2.3.1. *Small deformation with isotropic material*

The strain energy of the elastic beam is given by

$$U = \frac{1}{2}\int \epsilon_x \sigma_x\,\mathrm{d}V. \tag{15}$$

Neglecting the quadratic terms, the strain–displacement relation is given by

$$\epsilon_x = \frac{\partial \bar{u}}{\partial x} - y\frac{\partial^2 \bar{v}}{\partial x^2}, \tag{16}$$

where $\bar{u}$ and $\bar{v}$ are the displacements vector along the centroidal axis.

Assuming a linear stress–strain relation and substituting equation (16) into equation (15), one obtains

$$U = \tfrac{1}{2}EA\int_0^l (\partial \bar{u}/\partial x)^2\,\mathrm{d}x + \tfrac{1}{2}EI\int_0^l (\partial^2 \bar{v}/\partial x^2)^2\,\mathrm{d}x, \tag{17}$$

where E is Young's modulus, I is the moment of inertia and A is the cross-sectional area.

2.3.2. *Large deformation with isotropic material*

The strain–displacement relation including the quadratic terms is

$$\epsilon_x = \frac{\partial \bar{u}}{\partial x} - y\frac{\partial^2 \bar{v}}{\partial x^2} + \frac{1}{2}\left(\frac{\partial \bar{v}}{\partial x}\right)^2. \tag{18}$$

Substituting equation (18) into equation (15) yields

$$U = \frac{1}{2}EA\int_0^l \left[\left(\frac{\partial \bar{u}}{\partial x}\right)^2 \mathrm{d}x + \frac{\partial \bar{u}}{\partial x}\left(\frac{\partial \bar{v}}{\partial x}\right)^2 + \frac{1}{4}\left(\frac{\partial \bar{v}}{\partial x}\right)^4\right]\mathrm{d}x + \frac{1}{2}EI\int_0^l \left(\frac{\partial^2 \bar{v}}{\partial x^2}\right)^2 \mathrm{d}x. \tag{19}$$

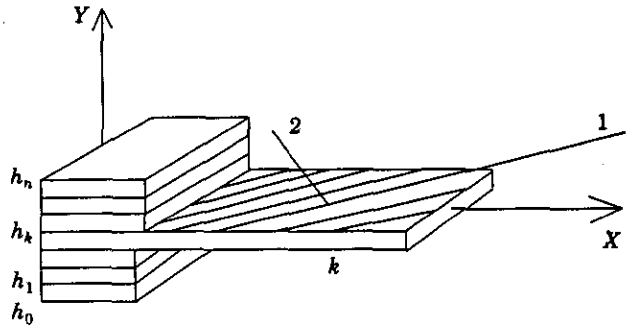

Figure 2. General configuration of the kth layer of the composite beam.

2.3.3. *Small deformation with composite material*

The general configuration of a composite beam is depicted in Figure 2. The relationship between stress and strain for a particular layer k in the local X–Y co-ordinate system can be expressed as

$$\begin{Bmatrix} \sigma_x \\ \sigma_y \\ \tau_{xy} \end{Bmatrix} = [\bar{\mathbf{Q}}]^{(k)} \begin{Bmatrix} \epsilon_x \\ \epsilon_y \\ \gamma_{xy} \end{Bmatrix}, \tag{20}$$

where the $[\bar{\mathbf{Q}}]^{(k)}$ matrix denotes the transformed reduced stiffness. The elements of $[\bar{\mathbf{Q}}]_{(k)}$ depend on the fiber angle between the local co-ordinate and the principle co-ordinate systems, as well as the engineering constant [44]. Based on classical lamination theory, the strain energy can be expressed by

$$U = \frac{1}{2}\int_0^l \left[A_{11}(\partial\bar{u}/\partial x)^2\,\mathrm{d}x + D_{11}\int_0^l (\partial^2\bar{v}/\partial x^2)^2 \right] \mathrm{d}x, \tag{21}$$

TABLE 1

Material properties and geometric parameters

Material properties	Graphite/epoxy	Steel
E_1 (Msi)	20	30
E_2 (Msi)	1·4	30
G_{12} (Msi	0·8	11·81
ν_{12}	0·3	0·27
h (in)	0·005	0·25
E/ρ (10^7 in)	33·33	10·6
ρ (lbm/in^3)	0·06	0·283
Geometric parameters, both materials		
Length	60 in	
Width	0·75 in	
Thickness	70·25 in	

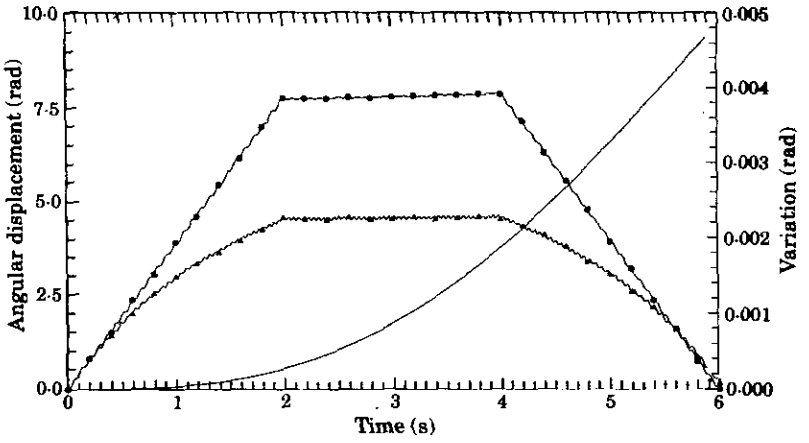

Figure 3. The angular displacement of the rotating steel beam: ——, rigid; ●–●–●–●, linear; ▲–▲–▲–▲, non-linear.

where

$$A_{11} = b \sum_{k=1}^{n} \bar{Q}_{11}^{(k)}(h_k - h_{k-1}), \qquad D_{11} = b \sum_{k=1}^{n} \tfrac{1}{3}\bar{Q}_{11}^{(k)}(h_k^3 - h_{k-1}^3) \tag{22}$$

with n pertaining to the number of layers; b is the width of the beam.

2.3.4. *Large deformation with composite material*

In a similar fashion, the strain energy can be expressed as

$$U = \frac{1}{2}\int_0^l \left[A_{11}\left(\frac{\partial \bar{u}}{\partial x}\right)^2 \mathrm{d}x + D_{11}\frac{\partial \bar{u}}{\partial x}\left(\frac{\partial \bar{v}}{\partial x}\right)^2 + \frac{1}{4}A_{11}\left(\frac{\partial \bar{v}}{\partial x}\right)^4 + A_{11}\int_0^l \left(\frac{\partial^2 \bar{v}}{\partial x^2}\right)^2 \right] \mathrm{d}x. \tag{23}$$

Substituting equation (6) into the strain energy equations (17), (19), (21) and (23), one can express the strain energy in terms of the generalized co-ordinate vector $\{\mathbf{q}_f\}$. By comparing the strain energy with the linear deformation and the geometric non-linear deformation, it can be realized that the two additional quadratic terms are attributed to geometric non-linear deformation. Shabaha [35] and Liou [36] neglected the fourth order term in the strain energy shown in equation (23) due to the tedious computations in the finite element approach. Following the procedure suggested in this paper, the fourth order term does not lead to very cumbersome computations, and is retained in the formulation.

2.4. GENERALIZED EXTERNAL FORCES

The principle of virtual work can be applied to derive the generalized external forces. The external forces in the rotating beam that can be considered in this study are the gravitational force and driving torque. However, any type of external force can be included following the same approach. The virtual work of all external forces acting on the beam can be written in matrix form as

$$\delta W = \{\mathbf{F}_e\}^{\mathrm{T}}\{\delta \mathbf{q}\} = [\mathbf{F}_{e\theta}, \{\mathbf{F}_e\}_f^{\mathrm{T}}] \begin{Bmatrix} \delta\theta \\ \delta q_f \end{Bmatrix}, \tag{24}$$

where $\mathbf{F}_{e\theta}$ and $\{\mathbf{F}_e\}_f^{\mathrm{T}}$ are generalized force vectors associated with the rigid and the elastic generalized co-ordinates, respectively.

The system equations of motion can be obtained by using Lagrange's formulation

$$\frac{\mathrm{d}}{\mathrm{d}t}\left(\frac{\partial T}{\partial \dot{\mathbf{q}}}\right)^{\mathrm{T}} - \left(\frac{\partial T}{\partial \mathbf{q}}\right)^{\mathrm{T}} + \left(\frac{\partial U}{\partial \mathbf{q}}\right)^{\mathrm{T}} = \mathbf{F}. \tag{25}$$

By performing the operations indicated in equation (25), the equations of motion can be expressed in matrix form

$$\begin{bmatrix} m_{\theta\theta}(\mathbf{q}, t) & m_{\theta f}(\mathbf{q}, t) \\ m_{f\theta}(\mathbf{q}, t) & m_{ff}(\mathbf{q}, t) \end{bmatrix} \begin{Bmatrix} \ddot{\theta} \\ \ddot{\mathbf{q}}_f \end{Bmatrix} + \begin{bmatrix} 0 & 0 \\ 0 & K_{ff} \end{bmatrix} \begin{Bmatrix} \theta \\ \mathbf{q}_f \end{Bmatrix} = \begin{Bmatrix} F_{e\theta}(\mathbf{q}, t) \\ F_{ef}(\mathbf{q}, t) \end{Bmatrix} + \begin{Bmatrix} Q_{v\theta}(\mathbf{q}, \dot{\mathbf{q}}, t) \\ Q_{vf}(\mathbf{q}, \dot{\mathbf{q}}, t) \end{Bmatrix}, \tag{26}$$

or in the concise form

$$[\mathbf{M}(\mathbf{q}, t)]\{\ddot{\mathbf{q}}\} + [\mathbf{K}]\{\mathbf{q}\} = \{\mathbf{F}_e(\mathbf{q}, t)\} + \{\mathbf{Q}_v(\mathbf{q}, \dot{\mathbf{q}}, t)\}, \tag{27}$$

where $\mathbf{Q}_v(\mathbf{q}, \dot{\mathbf{q}}, t)$ is the quadratic velocity vector resulting from differentiating the kinetic energy with respect to time and with respect to the body co-ordinates.

3. NUMERICAL RESULTS

A representative numerical example is provided in this section, to elucidate the relative significance of each model. The steel beam and the graphite/epoxy beam are selected to illustrate the performance of an isotropic and a composite material. The material

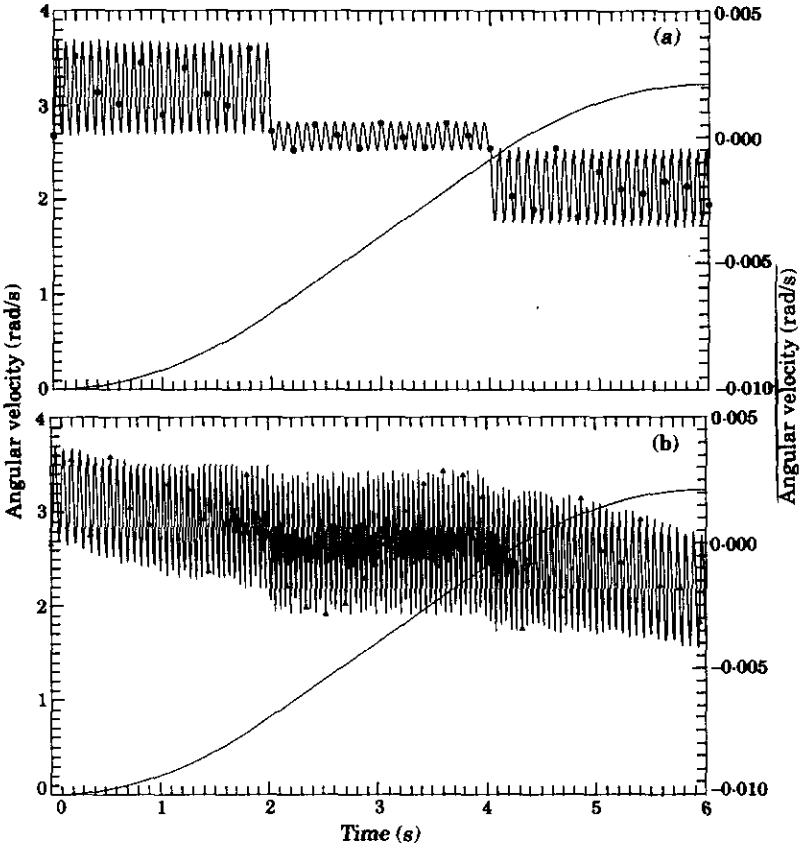

Figure 4. The angular velocity of the rotating steel beam. (a) ——, Rigid; ●–●–●–●, linear. (b) ——, Rigid; ▲–▲–▲–▲, non-linear.

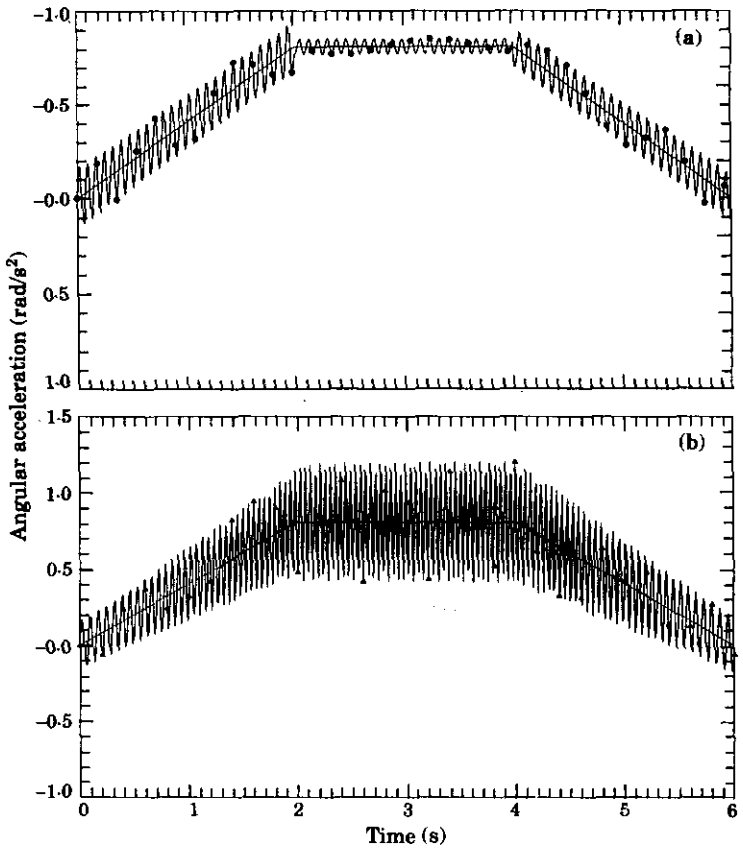

Figure 5. The angular acceleration of the rotating steel beam. (a) ——, Rigid; ●–●–●–●, linear. (b) ——, Rigid; ▲–▲–▲–▲, non-linear.

properties and the geometric parametric parameters of the beams are listed in Table 1, in which E_1 and E_2 are the Young's modulus in the 1- and 2-axis directions (defined in Figure 2), G_{12} is the shear modulus in the 1–2 plane and ν_{12} is the Poisson ratio for transverse strain in the 2-direction when stressed in the 1-direction. Both axial and transverse deformations, with one mode shape function, are considered.

Due to the coupled effect between rigid body motion and elastic deformation, the equations of motion are non-linear, the non-linearity being attributed to the dependency of the mass matrix on the time-dependent generalized elastic co-ordinates. In linear elastodynamics theory, the effects of the generalized elastic co-ordinates on the mass matrix are neglected such that the inverse dynamic analysis can be applied to a specific prescribed motion. However, this simplification can cause inaccuracy in simulating the dynamic behavior of the system. In order to maintain the equations of motion with the time variation of the mass matrix, the forward dynamic procedure is performed without any simplifications. The beam rotates under a prescribed torque in horizontal plane without any other external load. The prescribed torque is given by

$$T(t) = \begin{cases} 4t \text{ lb in}, & 0 \leqslant t \leqslant 2, \\ 8 \text{ lb in}, & 2 \leqslant t \leqslant 4, \\ 8 - 4t \text{ lb in}, & 4 \leqslant t \leqslant 6, \end{cases}$$

and the total simulation time is 6 seconds. A small integration time step must be selected in order to obtain an accurate solution for such type of stiffened system. The predictor–corrector Adams-Bashforth-Moulton algorithm is used in this example [45].

The responses in terms of angular displacement, velocity and acceleration of the steel beam in rigid motion, linear small deformation, and geometric non-linear deformation are shown in Figures 3 to 5, respectively. The corresponding responses of the graphite/epoxy beam are shown in Figures 6 to 8. The influences of flexibility on the angular displacement and velocity are minimal. It is convenient to illustrate the results of Figures 3, 4, 6 and 7 individually. The left-hand y-axis indicates the rigid motion response and the right-hand y-axis indicates the variations between flexible and rigid motion. The high frequency responses of angular velocity and angular acceleration are due to the effect of high stiffness of the beam. It is observed that, as shown in Figure 3, the total angular displacement of the steel beam is about one and half revolutions. On the contrary, the total angular displacement of the graphite/epoxy beam is about seven revolutions. Less energy consumption is required for composite beam if the same angular displacement occurs. This is because the steel beam has a much higher mass density and the angular displacement for a given torque is inversely proportional to mass density. The mass density of steel is $0{\cdot}283/0{\cdot}06 = 7{\cdot}717$ times greater than that of graphite/epoxy. The angular displacements of the steel and the graphite/epoxy beam are 1·5 and 7 revolutions, respectively. As a matter of fact, $7/1{\cdot}5 = 4{\cdot}667$ is essentially the same as the mass density ratio of 4·717. Therefore, the effect of the elastic deformations on the moment of inertia is small. The flexibility affects the angular acceleration, especially for geometric non-linearity deformation motion for both materials. The sources of angular acceleration oscillations come from the Coriolis acceleration $Q_{v\theta}$ and the inertial forces $[m_{\theta f}]\{\ddot{q}_f\}$ (see equation (26)). It is worth mentioning that the generalized co-ordinates θ are related to the rigid body motion.

As shown in Figures 9 and 10, the transverse deformations are dominated by a forcing function which is mainly caused by the inertia input torque [24]. In the LI modelling shown in Figures 5 and 9, the beam, subjected to a maximum angular acceleration of 0·8 rad/s^2, experiences a maximum deformation of 0·28 in. However, in the LCP modelling shown in Figures 8 and 10, the corresponding angular acceleration and maximum deformation are 4 rad/s^2 and 0·45 in. The angular acceleration from the LCP model is five times higher than

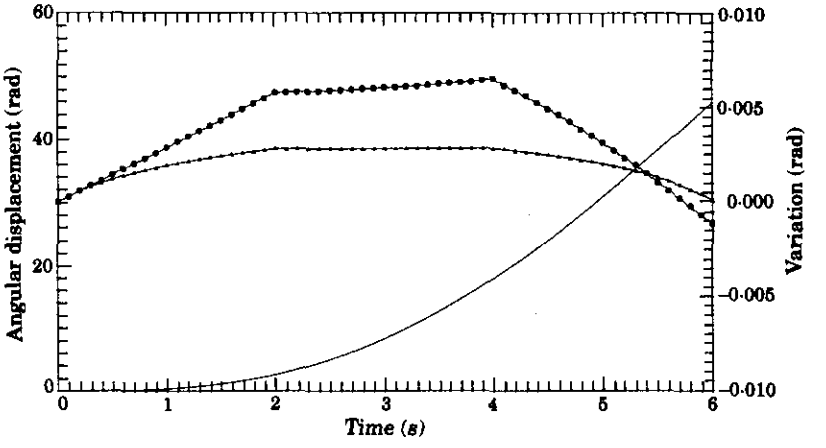

Figure 6. The angular displacement of the rotating graphite/epoxy beam: ——, Rigid; ●–●–●–●, linear; ▲–▲–▲–▲, non-linear.

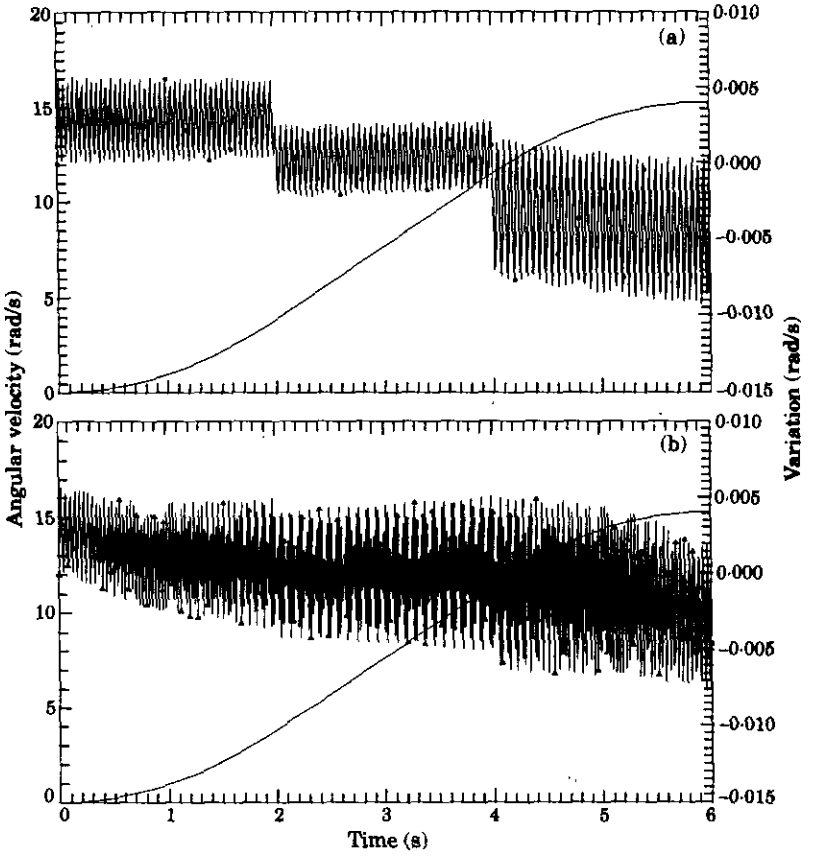

Figure 7. The angular velocity of the rotating graphite/epoxy beam. (a) ——, Rigid; ●-●-●-●, linear. (b) ——, Rigid; ▲-▲-▲-▲, non-linear.

that of the LI model, but the maximum deformation is about twice as great as that from the LI model. This can be attributed to the high stiffness-to-weight ratio in composite materials. Passive control in damping the vibration of the structure can be achieved when composite material is selected. The maximum deformation in the linear deformation model is about 50 percent greater than in the geometric non-linearity deformation model, for both materials. Therefore, the correct mathematical model is indispensable for a more accurate analysis of realistic flexible structure systems.

4. CONCLUSIONS

Comparative modelling of a flexible rotating beam has been studied in this paper. The dynamic models describe a beam with isotropic material and composite material, subjected to small linear deformation and geometrical non-linearity deformation, respectively. The composite beam is considered as orthotropic fiber-reinforced and symmetrically laminated. The methodology is applied to the study of different model combinations: (a) linear deformation with isotropic material (LI); (b) geometric non-linearity deformation with isotropic material (NLI); (c) linear deformation with composite material (LCP); and (d) geometric non-linear deformation with composite material (NLCP).

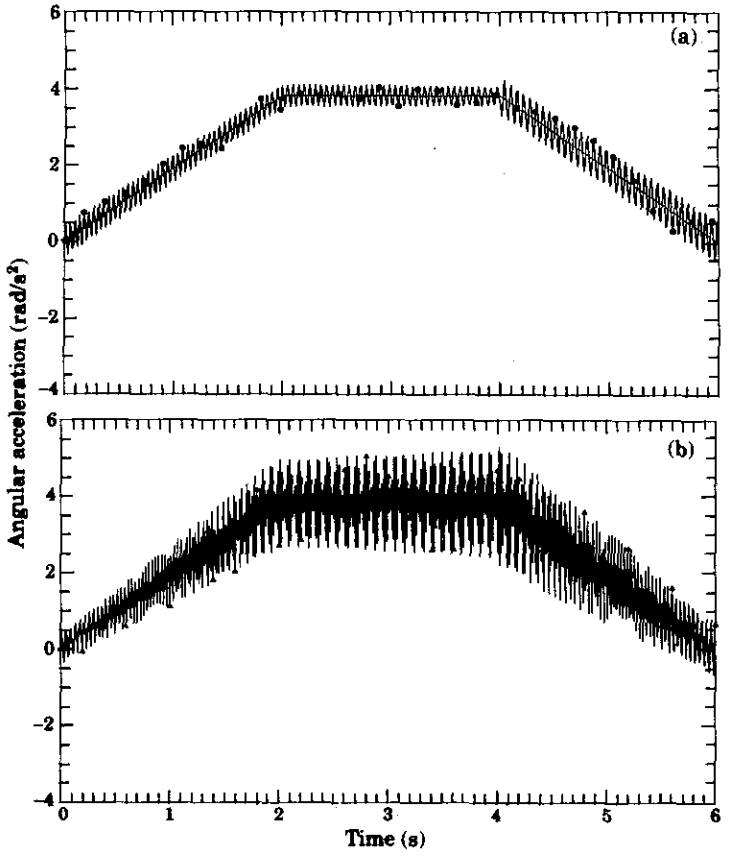

Figure 8. The angular acceleration of the rotating graphite/epoxy beam (a) ——, Rigid; ●–●–●–●, linear. (*b*) ——, Rigid; ▲–▲–▲–▲, *non-linear.*

The coupled effect between the rigid body motion and the flexible motion is also considered. The equations of motion are non-linear with time-dependent coefficients. They are expressed in terms of the elastic generalized co-ordinates and the large angular displacement of the beam. The forward numerical simulation is performed for a prescribed torque driving the steel and graphite/epoxy beam. The transverse deformation responses

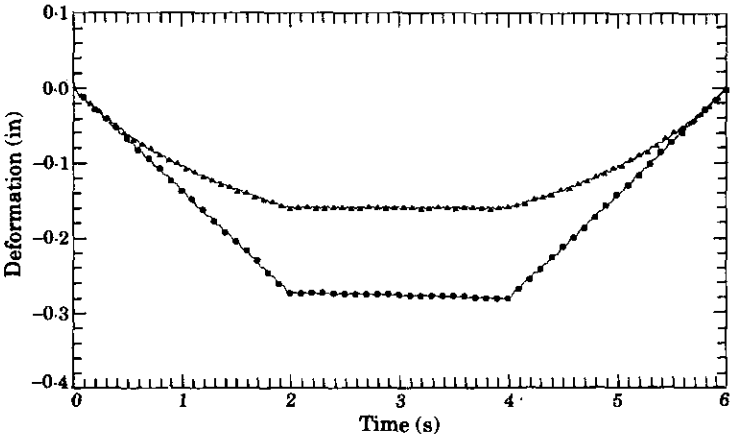

Figure 9. The end-point deformation of the rotating steel beam: ●–●–●–●, *linear;* ▲–▲–▲–▲, *non-linear.*

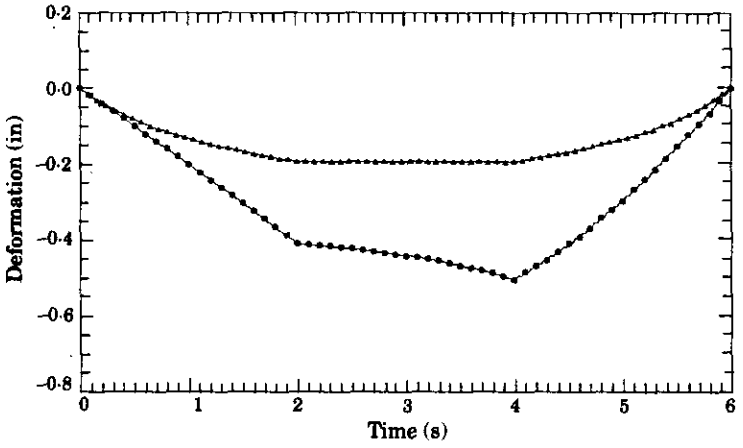

Figure 10. The end-point deformation of the rotating graphite/epoxy beam: ●-●-●-●, linear; ▲-▲-▲-▲, non-linear.

and the influence of flexibility on the rigid body motion are evaluted and discussed. For the composite material, it is shown that it has lower energy consumption due to lower material density. It performs well in damping the vibration of the structure, due to its higher stiffness-to-weight ratio.

REFERENCES

1. M. BADLAN, W. KLEINHENZ and C. C. HSIAO 1978 *Mechanism and Machine Theory* **13**, 555–564. On vibration of rotating shaft.
2. S. V. HOA 1979 *Journal of Sound and Vibration* **67**, 369–381. Vibration of a rotating beam with tip mass.
3. Y. P. MITCHELL JR. and J. C. BRUCH 1988 *Transactions of the American Society of Mechanical Engineers, Journal of Vibrations, Acoustics, Stress and Reliability in Design* **110**, 118–120. Free vibrations of a flexible arm attached to a compliant finite hub.
4. T. YOKOYAMA 1988 *International Journal of Mechanical Science* **30**, 743–755. Free vibration characteristics of rotating Timoshenko beams.
5. H. F. BANER and W. EIDEL 1988 *Journal and Sound and Vibration* **122**, 357–375. Vibration of rotating uniform beam, part II: orientation perpendicular to the axis of rotation.
6. M. C. DELFOUR, M. KEM, L. PASSERON and B. SECENNEC 1986 *IFAC Symposium on Control of Distributed Parameter Systems, Los Angeles, California*, 383–387. Modeling of rotating flexible beam.
7. J. C. SIMO and L. VU-QUOC 1986 *Transactions of the American Society of Mechanical Engineers, Journal of Applied Mechanics* **53**, 849–854. On the dynamics of flexible beam under large over all motions—the plane case: part 1.
8. J. C. SIMO and L. VU-QUOC 1986 *Transactions of the American Society of Mechanical Engineers, Journal of Applied Mechanics* **53**, 855–861. On the dynamics of flexible beam under large over all motions—the plane case: part 2.
9. A. A. GOLDENBERG and F. RAKHSHA 1986 *Mechanism and Machine Theory* **21**, 325–335. Feedforward control of a single-link flexible robot.
10. J. D. LEE and B.-L. WANG 1988 *Computers and Structures* **29**, 459–467. Optimal control of a flexible robot arm.
11. G. G. LOWEN and C. CHASSAPIS 1986 *Mechanism and Machine Theory* **21**, 33–42. The elastic behavior of linkages: an update.
12. K. H. LOW 1987 *Journal of Robotic Systems* **4**, 435–456. A systematic formulation of dynamic equations for robotic manipulators with elastic links.

13. K. H. Low and M. Vidyasagar 1988 *Transactions of the American Society of Mechanical Engineers, Journal of Dynamic Systems, Measurement and Control* **110**, 175–181. A Lagrangian formulation of the dynamic model for flexible manipulator systems.
14. A. A. Shabana 1989 *Dynamic of Multibody Systems*. New York: John Wiley.
15. T. E. Blejwas 1981 *Mechanism and Machine Theory* **16**, 441–445. The simulation of elastic mechanisms using the kinematic constraints and Lagrange multipliers.
16. A. Midha, A. G. Erdman and D. A. Frohrib 1977 *Journal of Engineering for Industry* **99**, 449–455. An approximate method for the dynamic analysis of elastic linkages.
17. B. M. Bahgat and K. D. Willmert 1976 *Mechanism and Machine Theory* **11**, 47–71. Finite element vibrational analysis of planar mechanisms.
18. W. L. Cleghorn and R. G. Fenton 1981 *Mechanism and Machine Theory* **16**, 407–424. Finite element analysis of high-speed flexible mechanisms.
19. C. I. Chen, V. H. Mucino and K. H. Means 1987 *Proceedings of Oklahoma State University's 10th Applied Mechanisms Conference, New Orleans, Louisiana*. A Lagrange-multiplier numerical solution to the elastio-dynamic response of flexible linkages.
20. V. H. Mucino, C. I. Chen and N. T. Sivaneri 1987 *Proceedings of Oklahoma State University's 10th Applied Mechanisms Conference, New Orleans, Louisiana*. A continous based Hamilton–Lagrange approach to the elasto-dynamics of flexible mechanisms.
21. M. Badlani and A. Midha 1983 *Transactions of the American Society of Mechanical Engineers, Journal of Mechanisms, Transmissions, and Automation in Design* **105**, 452–459. Effect of internal material damping of the dynamics of a slider–crank mechanism.
22. P. K. C. Wang and J.-D. Wei 1987 *Journal of Sound and Vibration* **116**, 149–160. Vibrations in a moving flexible robot arm.
23. V. Masurekar and N. K. Gupta 1988 *Mechanism and Machine Theory* **23**, 367–375. Stability analysis of four bar mechanism, part I—taking damping into consideration.
24. C. I. Chen 1992 *Ph.D. Dissertation, College of Engineering, West Virginia University*. Three dimensional elastodynamic modeling and analysis of a flexible robot manipulator.
25. E. R. Christensen and S. W. Lee 1986 *Computers and Structures* **23**, 819–829. Nonlinear finite element modeling of the dynamics of unrestrained flexible structures.
26. F. Van Der Ween 1988 *Mechanism and Machine Theory* **23**, 491–500. A finite element approach to three-dimensional kineto-elastodynmics.
27. W. L. Cleghorn and K. C. Chao 1988 *Mechanism and Machine Theory* **23**, 333–342. Kineto-elastodynamic modelling of mechanisms employing linearly tapered beam finite elements.
28. Z. Yang and J. P. Sadler 1990 *Transactions of the American Society of Mechanical Engineers, Journal of Mechanical Design* **112**, 175–182. Large-displacement finite element analysis of flexible linkages.
29. P. Kalra and A. M. Sharan 1991 *Mechanism and Machine Theory* **26**, 299–313. Accurate modeling of flexible manipulators using finite element analysis.
30. A. A. Shabana and R. A. Wehage 1993 *Transactions of the American Society of Mechanical Engineers, Journal of Mechanisms, Transmissions, and Automation in Design* **105**, 391–378. Variable degree-of-freedom component mode analysis of inertia variant flexible mechanical systems.
31. A. A. Shabana and R. A. Wehage 1984 *Transactions of the American Society of Mechanical Engineers, Journal of Mechanisms, Transmissions, and Automation in Design* **106**, 172–106. Spatial transient analysis of inertia-variant flexible mechanical systems.
32. B. S. Thompson and C. K. Sung *ASME* 84-*DEC*-15. A variational formulation for nonlinear finite element analysis of flexible linkages.
33. D. A. Turcic and A. Midha 1984 *Transactions of the American Society of Mechanical Engineers, Journal of Dynamic Systems, Measurements and Control* **106**, 249–254. Dynamic analysis of elastic mechanism systems, part I: applications.
34. D. A. Turcic and A. Midha 1984 *Transactions of the American Society of Mechanical Engineers, Journal of Dynamic Systems, Measurements and Control* **106**, 255–260. Dynamic analysis of elastic mechanism systems, part II: experimental results.
35. E. K. Bakr and A. A. Shabana 1986 *Computers and Structures* **23**, 739–751. Geometrically nonlinear analysis of multi-body systems.
36. F. W. Liou and A. G. Erdman 1989 *Transactions of the American Society of Mechanical Engineers, Journal of Vibration, Acoustics, Stress, and Reliability in Design* **111**, 35–41. Analysis of a high speed flexible four-bar linkage: part I—formulation and solution.
37. B. S. Thompson, D. Zuccaro, D. Gamache and M. V. Gandhi 1983 *Mechanism and Machine Theory* **18**, 165–171. An experimental and analytical study of a four bar mechanism.

38. C. K. SUNG and B. S. THOMPSON 1984 *Mechanism and Machine Theory* **19**, 389–396. Material selection: an important parameter in design of high-speed linkages.
39. B. S. THOMPSON and C. K. SUNG 1984 *Transactions of the American Society of Mechanical Engineers, Journal of Mechanisms, Transmissions, and Automation in Design* **106**, 183–190. A variational formulation for the dynamic viscoelastic finite element analysis of robotic manipulators constructed from composite materials.
40. B. S. Thompson and C. K. Sung 1986 *Journal of Sound and Vibration* **111**, 399–428. An analytical and experimental investigation of high-speed mechanisms fabricated with composite laminates.
41. A. A. SHABANA 1986 *Journal of Sound and Vibration* **108**, 487–502. Effect of using composites on the dynamic response of multi-body systems.
42. J. G. D'ACQUISTO 1988 *M.S.M.E. Thesis, College of Engineering, West Virginia University*. Helically wound composites for performance enhancement of flexible linkages.
43. K. KRISHNAMURTHY, K. CHANDRASHEKHARA and S. ROY 1990 *Computers and Structures* **36**, 139–146. A study of single-link robots fabricated from orthotropic composite materials.
44. R. M. JONES 1975 *Mechanics of Composite Materials*. New York: McGraw-Hill.
45. C. W. GEAR 1971 *Numerical Initial Value Problems in Ordinary Differential Equations*. Englewood Cliffs, NJ: Prentice Hall.